EFFECT OF SHORT-TERM WATER EXPOSURE ON MECHANICAL PROPERTIES OF MULTI-LAYER GRAPHENE AND MULTI-WALLED CARBON NANOTUBES-REINFORCED EPOXY NANOCOMPOSITES

MOHD SHAHNEEL SAHARUDIN[1,*], SYAFAWATI HASBI[2],
NASRIZAL MOHD RASHIDI[3], MOHD SHAHAREL JAMAL NORDIN[1]

[1]Universiti Kuala Lumpur Malaysia Italy Design Institute (UniKL MIDI),
119 Jalan 7/91, Taman Shamelin Perkasa, 56100, Kuala Lumpur, Malaysia
[2]Department of Mechanical Engineering, Faculty of Engineering, National Defense,
University of Malaysia (NDUM), Kem Sungai Besi, 57000, Kuala Lumpur, Malaysia
[3]Universiti Kuala Lumpur Malaysia France Institute (UniKL MFI), Section 14 Jalan Teras,
Jernang, 43650, Bandar Baru Bangi, Selangor, Malaysia
*Corresponding Author: mshahneel@unikl.edu.my

Abstract

The influence of short-term water absorption on the mechanical properties of Multi-Layer Graphene (MLG) and Multi-Walled Carbon Nanotubes (MWCNTs) reinforced epoxy hybrid nanocomposites were studied. Water absorption test was conducted by immersing specimens in water at room temperature for 96 hours. The lowest water absorption was 0.4% in the case of 0.1 wt% MLG-epoxy. The highest improvement of Young's modulus and tensile strength were observed in the case of 0.1 wt% MLG-epoxy, where the value increased to 72.4% and 58% respectively. After water immersion, Young's modulus and tensile strength dropped 6.7% and 29% compared to the dry samples. The fracture toughness of 0.1 wt%-epoxy increased up to 113% for dry samples. After water exposure, the fracture toughness increased to 125% due to the plasticisation effect of the resin matrix. Findings showed that MLG has great influence in enhancing the mechanical performances of epoxy nanocomposites than MWCNTs. It was also observed that synergistic effects are not effective to produce significant improvement in mechanical properties of produced hybrid nanocomposites at the concentration of 0.1 wt%.

Keywords: Carbon nanotubes, Epoxy, Graphene, Mechanical properties, Water absorption.

1. Introduction

Epoxy is a widely used thermoset material in aerospace, automotive and marine applications owing to its superior mechanical properties, thermal stability, solvent resistance and ease of processing [1-4]. Polymer composites with carbon nano-fillers have many potential applications, which include thermal management, electronics, fuel cells and transportation [5, 6]. Mechanical properties of the polymer can be improved with the addition of carbon-based filler such as graphene and Carbon Nanotubes (CNTs) [7, 8]. Graphene, a single layer of graphite, is a material that chemically stable and electrically conducting membrane one atom in thickness [9]. Recently, graphene has gained interest from industry because of its outstanding properties, that include high surface to volume ratio, high aspect ratio, extremely low electrical resistivity, high thermal conductivity and high mechanical strength and modulus [10-12]. Wei et al. [13] commented that their excellent properties have fascinated research in recent years with ever-increasing scientific and technological impetus. Based on our previous research, a significant improvement in Young's modulus and fracture toughness was observed in the case of 0.1 wt% MLG-epoxy system [14]. The increase in stiffness and restriction in the movement of polymer chains by 0.1 wt% of MLG has been reported in another publication [11].

CNTs, on the other hand, were discovered accidentally by Ijima in 1991 [15]. CNTs were formed at the cathode during sputtering of graphite by an electronic arc and derived nanotubes were identified as Multi-Walled Carbon Nanotubes (MWCNTs). Carbon Nanotubes (CNTs) are known as one of the stiffest engineering fibres [16, 17]. Based on studies by Inam and Luhyna [18], these materials have great potential as nano-fillers for aerospace application due to their unique combination of chemical and physical properties event at very small size. CNTs have tensile strengths significantly higher than steel and carbon fibre, electrical conductivity similar to silver and platinum and capable of carrying higher current densities than copper. They also have better thermal conductivity than diamond and lower density than aluminium [19]. The hybrid nanocomposite is normally used to suit requirements and to offset the disadvantages of one component by the addition of another [18]. Previous research in this area was focusing on properties of hybrid micro-composites in which, dispersed second phase nanoparticles are added to the epoxy matrix. In this research, we prepared hybrid nanocomposites based on multi-layer graphene, multi-walled carbon nanotubes and epoxy matrix, which then exposed to water immersion (96 h).

In some applications, the contact between polymeric materials and the liquid environment is unavoidable and may lead to catastrophic failure. The failure is caused by the liquid absorption and swelling of the polymer matrix as it interacts with the penetrating liquid environment [20]. The liquid absorption can be reduced by using carbon base nano-fillers such as Multi-Layer Graphene (MLG) and Multi-Walled Carbon Nanotubes (MWCNTs). According to Sumfleth et al. [21], the addition of hybrid nano-fillers improves dispersion states of MLG and CNT in the polymer matrix and help to improve the physical properties of hybrid nanocomposites as the synergistic effects become active. A remarkable synergetic effect between MGPs and MWCNTs on the enhanced mechanical properties and thermal conductivity of these composites was also demonstrated in other publications [22, 23]. Although various studies have been carried out on mechanical properties of hybrid composites, there is an obvious gap in the literature

in discussing the effect of short-term water exposure on the mechanical properties hybrid nanocomposites. The objective of this research is to determine whether the hybrid nanocomposites could have a remarkable synergistic effect both for dry and immersed samples.

2. Methodology

2.1. Materials

Multi-Layer Graphene (MLG) of 12 nm average thickness and 4.5 μm average lateral size with a surface area of 80 m^2/g and purity 99.2% was purchased from Graphene Supermarket, USA. Multiwalled carbon nanotubes (MWCNTs) supplied by S. Elements, Waalre, Netherlands was used as second filler. The inter-shell spacing between tubes is between 0.344 nm to 0.36 nm and the carbon bond length is 0.144 nm. The epoxy and hardener used in this research are Miracast 1517A and Miracast 1517B supplied by Miracon Sdn. Bhd., Seri Kembangan, Malaysia. The epoxy has a density of 1.13 g/cm^3 while the hardener has 1.1 g/cm^3 density. This epoxy system is a standard resin for composite industry and has low viscosity. The low viscosity of the hardener helps to improve the dispersion state and the fast curing to prevent the reinforcement agglomeration. The gelation time of the resin was 40 min at Room Temperature (RT).

Composites preparation

Epoxy resin was thoroughly mixed with hardener at a ratio of 2: 1 and was vacuum degassed for 10 minutes. The mixture then poured into moulds for curing at room temperature for 12 h. Then, the post-curing process at 120 ℃ was carried out on the samples for another 14 h. For hybrid samples, the MLG (0.05 wt%) and MWCNTs (0.05 wt%) were taken and dispersed in epoxy at room temperature for 10 minutes. The reinforcement dispersed epoxy and hardener were then vacuum degassed separately for another 10 minutes. Next, the hardener was mixed in epoxy: hardener ratio of 2 : 1. Following thorough hand mixing for 10 minutes, vacuum degassing was carried out for another 10 minutes. The resin was poured into moulds and cured at room temperature for 12 h followed by post-curing at 120 °C for 14 h as recommended by the supplier (Miracon Sdn. Bhd.) to ensure complete crosslinking. The similar procedures were carried out for 0.1 wt%-MLG epoxy and 0.1 wt%-MWCNTs epoxy.

2.2. Characterization of composites

Rectangular specimens with dimensions 80 x 10 x 4 mm were immersed into water at room temperature for 96 h. There is no standard to determine the duration of immersion, however, 96 h can be considered as short-term immersion based on available studies [12, 24]. As reported by Faruk et al. [25] and Alamri and Low [26] in their publications, several studies have longer immersion time such as 150 days and 130 days. The weight was measured using 0.001 mg weighing balance. Before weighing process, the surface of the specimen was wiped with tissue paper. The water absorption percentage was calculated based on the weight increase in the samples. Equation (1) was used to measure the water absorption in the specimens, where W_t is the weight of specimen at time t (i.e., after immersion in the water) and W_o is the initial weight of the sample, i.e., before placing in water.

$$Wc = (W_t - W_0) \times \frac{100}{W_0} \tag{1}$$

A tensile test was performed using Victor Universal Testing Machine (Victor VE 2302). Five specimens were tested for each composition. The displacement rate for the tensile tests was kept to 1 mm/min. Tensile test properties were carried out according to ISO 527 with a specimen thickness of 3 mm. Figure 1 shows the illustration of samples used in the tensile test, impact test and fracture toughness test.

The fracture toughness (K_{1C}) was obtained using a Single Edge Notch Three-Point Bending (SEN-TPB) specimen (ASTM D5045). The displacement rate used was 1 mm/min. The dimensions were $3 \times 6 \times 36$ mm^3 with a crack length of 3 mm at the centre of the sample. K_{1C} was calculated using linear fracture mechanics by following relationship Eq. (2). The calibration factor used is presented in Eq. (3).

$$K_{1C} = \frac{P_{max}(\frac{a}{w})}{BW^{1/2}} \tag{2}$$

where $f(a/w)$ is the calibration factor for the samples, which is given as:

$$f\left(\frac{a}{w}\right) = \frac{[(2+\frac{a}{w})\{0.0866+4.64(\frac{a}{w})^2+14.72(\frac{a}{w})^3-5.6(\frac{a}{w})^4]}{(1-\frac{a}{w})^{3/2}} \tag{3}$$

Charpy impact toughness test was carried out according to ISO 178 with dimensions of $80 \times 10 \times 4$ mm. The impact toughness was obtained using equation (3), where m is mass of hammer (kg), g is standard gravity (9.81 ms^{-2}), h is the length of the hammer (m) and is sample thickness (mm). Thus;

$$\text{Impact strength} = \frac{mgh\ (\cos\beta - \cos\alpha)}{wt} \tag{4}$$

The average surface roughness R_a was measured using portable Surface Roughness Tester (Mitutoyo SURFTEST SJ-210) and comply with ISO1997 standard. R_a is commonly adopted in general engineering practice. This standard gives a good narrative of the height variations in the surface of measured specimens.
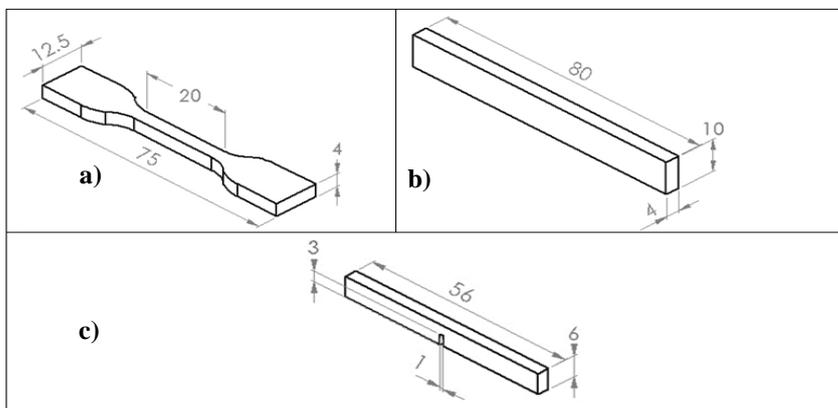

Fig. 1. Illustration of samples (a) tensile,
(b) impact strength, and (c) fracture toughness K_{1C}.

3. Results and Discussion

3.1. Maximum water absorption

Figure 2 shows the maximum water absorption of the nanocomposites. The highest absorption was observed in the case of Monolithic Epoxy (ME), with 2.5%. For 0.1 MWCNTs-epoxy nanocomposites, the water absorption was 1.6%. For 0.05 wt% MLG-0.05 wt% MWCNTs the water absorption was 1.5%. The lowest value was observed in the case of 0.1 wt% MLG-epoxy nanocomposites, where 0.4% of water absorption was recorded. Composites that contained fillers with high aspect ratio can impede and alter the diffusion path of penetrating molecules. A similar trend could be observed in the case of hybrid nanocomposites and 0.1 wt% MLG-epoxy nanocomposites. The fillers create a tortuous path for permeants to travel [27] and as a result, the maximum water absorptions were decreased for all nanocomposite systems. The tortuosity path created by the filler particles in a polymer force caused the water molecule to travel further around the filler particles. Tortuosity, also causing a physical blocking effect as the filler forces the diffusant to take a more indirect, or additional path through the composite materials [28].

Including model by Cussler et al. [29] and Fredrickson and Bicerano [30], there are numerous models that have been proposed to show the effect of nanofillers in reducing water permeability through polymers. The degree of tortuosity imposed is dependent upon the anisotropy and orientation of the filler particles with respect to the direction of diffusion [31]. In addition, at room temperature graphene is practically impermeable to all molecules as mentioned by several researchers [27, 32, 33]. Water clustering and agglomeration effects can occur to influence moisture barrier properties of polymer nanocomposites. Tan and Thomas [32] have reported that water clustering causes a reduction in water diffusivity and tends to occur in hydrophobic polymers and in the neighbourhood of nano-platelets. However, in our case, water clustering effect was not observed. In our research, the agglomeration effect can be ruled out as there is no evidence from SEM analysis. It is apparent that in this research, water entering nanocomposites through capillarity and caused plasticisation.
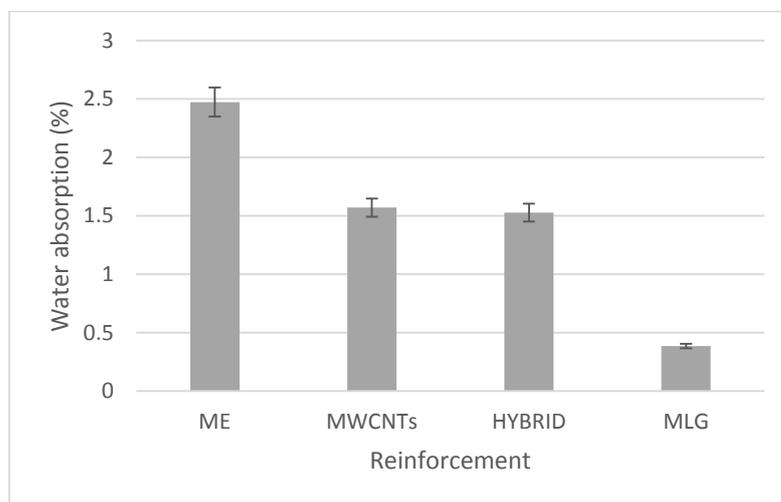

Fig. 2. Water absorption test.

3.2. Force versus time graph

Figures 3(a) and (b) show the force versus time curves for all nanocomposite systems. Samples reinforced with 0.1 wt% MLG-epoxy have the highest value of force followed by hybrid composite and 0.1 wt% MWCNTs-epoxy. For samples exposed in water, the time to failure increased compared to unexposed samples. This is due to plasticisation effect on nanocomposites and the change from brittle to ductile failure, which can be associated with resin plasticisation by water sorption and cross-link breaking [34]. Water had penetrated into the resin and plasticiser effect is observed [20, 35]. Water diffused along the particle-matrix interface degrades the interfacial bond strength hence, contributing to the loss of structural integrity [36].
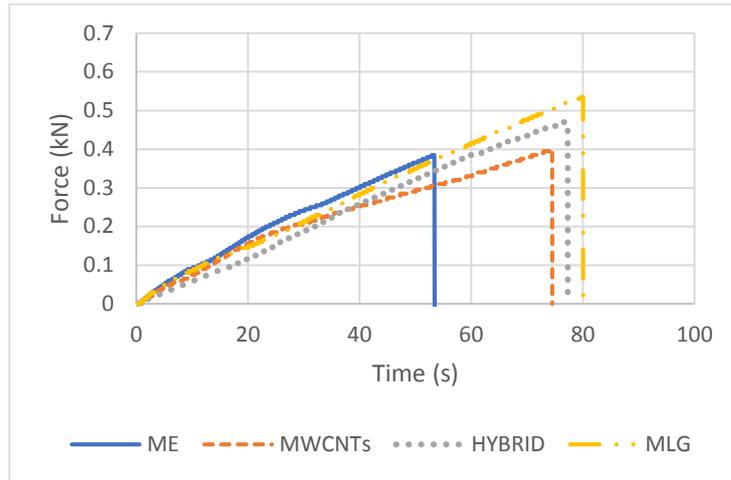
(a)
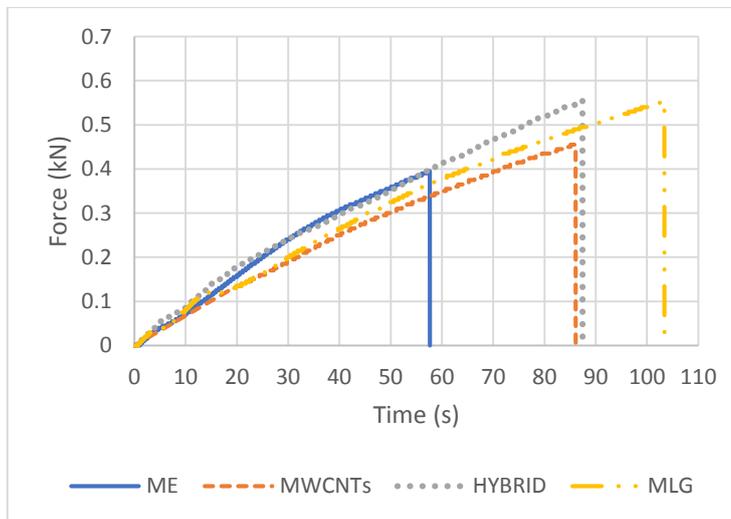
(b)

Fig. 3. Force-time curves of:
(a) dry samples (b) samples after water exposure.

3.3. Tensile properties

Figure 4 shows the Young's modulus of nanocomposites before and after water exposure. It can be seen that monolithic epoxy recorded the lowest Young's modulus with just 0.87 GPa, compared to other dry samples. The Young's modulus increased from 0.87 GPa to 1.4 GPa (increased 61%) in the case of 0.1 wt% MWNTs-epoxy. For hybrid samples, the Young's modulus increased by 70%. The highest improvement of Young's modulus was in the case of 0.1 wt% MLG-epoxy nanocomposites, where the value increased by 72.4%. After water exposure, the Young's modulus decreased for all nanocomposite systems. Compared to dry samples, the Young's modulus of monolithic epoxy decreased 9%. For hybrid samples, the Young's modulus decreased by 5.4% and in the case of 0.1 wt% MLG-epoxy, the Young's modulus dropped 6.7%.

Figure 5 shows the tensile strength of dry and immersed composite samples. Monolithic epoxy recorded the lowest tensile strength compared to nanocomposites tested in dry condition. A remarkable improvement was achieved in the case of 0.1 wt% MLG-epoxy, where the tensile strength improved by 58%. This was attributed to the large aspect ratio of the graphene sheets and the strong interfacial adhesion between graphene and epoxy matrix [37].

For hybrid nanocomposite samples, the tensile strength increased by 29%, which is half of what has been achieved in 0.1 wt% MLG-epoxy system. After water exposure, the tensile strength for all specimens slightly decreased compared to samples tested in dry condition. The tensile strain of all nanocomposite systems is presented in Fig. 6. For dry samples, the highest tensile strain value was observed in the case of monolithic epoxy, followed by 0.1 wt% MWNTs-epoxy, hybrid samples and 0.1 wt% MLG-epoxy. After water exposure, the tensile strain percentages increased for monolithic epoxy and all nanocomposites. For instance, the tensile strain of monolithic epoxy increased from 3.6% to 4.1%. Figure 7 shows fracture toughness of dry and immersed samples. The highest fracture toughness in both cases were observed in the case of 0.1 wt% MLG-epoxy. After water exposure, the fracture toughness increased for all samples. This is due to the plasticization effect, which leads to ductile failure in the matrix.
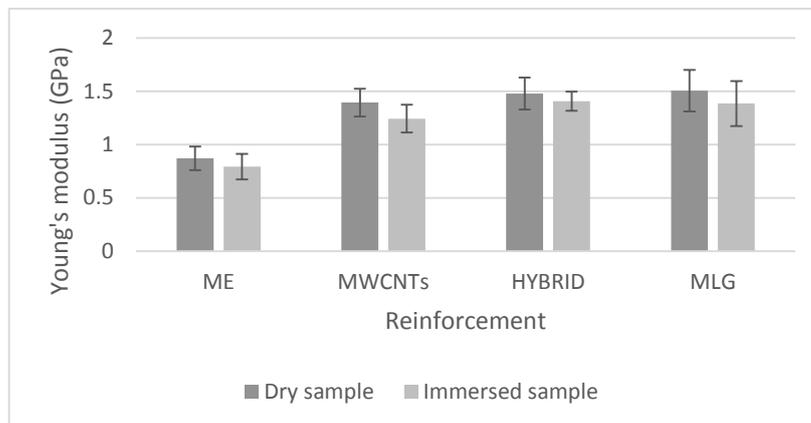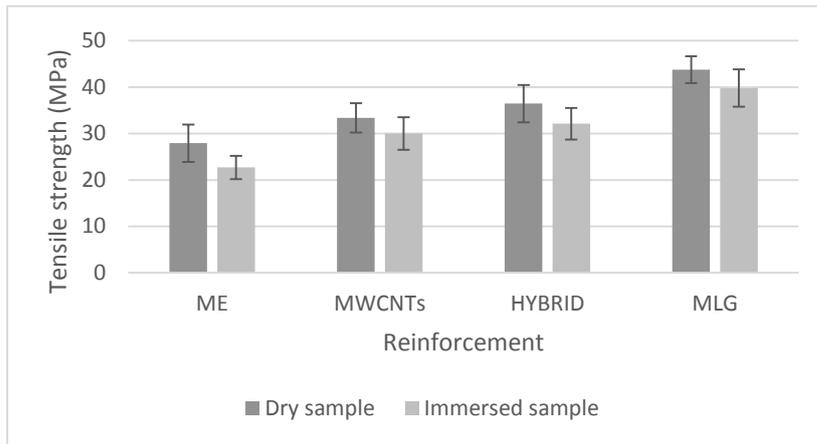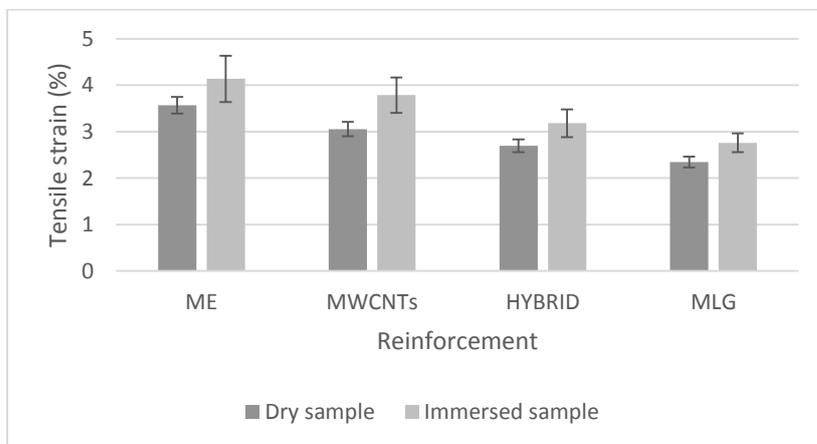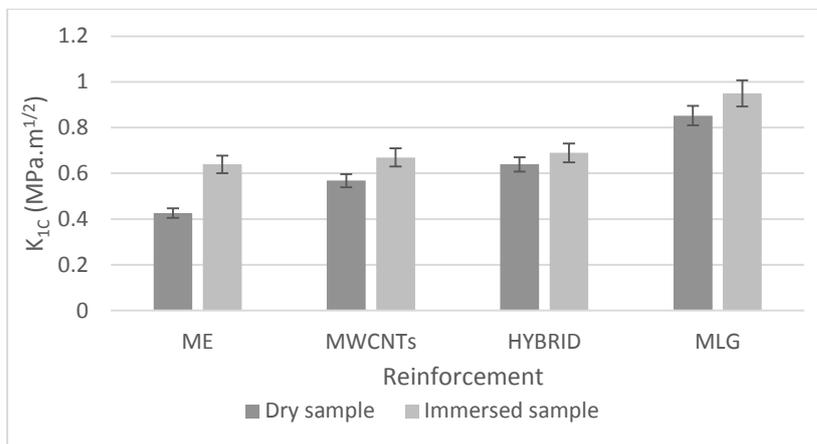

Fig. 4. Young's modulus of dry and immersed samples.

Fig. 5. Tensile strength of dry and immersed samples.

Fig. 6. Tensile strain of dry and immersed samples.

Fig. 7. Fracture toughness of dry and immersed samples.

3.4. Surface roughness

The surface roughness of nanocomposites is shown in Fig. 8. For dry samples, 0.1 wt% MLG-epoxy nanocomposites recorded the highest surface roughness with 1.8 μm followed by hybrid nanocomposites with 1.7 μm. After water exposure, the surface roughness slightly increased for all nanocomposite systems. Hybrid nanocomposites recorded an increase of 26%. In the case of 0.1 wt% MLG-epoxy, the surface roughness increased 46%. A high contact area between polymer and nanofiller maximises stress transfer from the polymer matrix to nanofillers. From the results obtained, 0.1 wt% MLG-epoxy shows better reinforcement than 0.1 wt% MWCNTs-epoxy simply because of their high aspect ratio, which is between 600-10000 [28, 38]. In the case of 0.1 wt% MLG-epoxy, when cracks formed, it deflects much, and rest of the fractured surface indicates the presence of deep surface notches, which is responsible for the increasing of R_a value. Apart from that, MLG also has a higher contact surface area compared to MWCNTs as reported in the literature [39, 40].
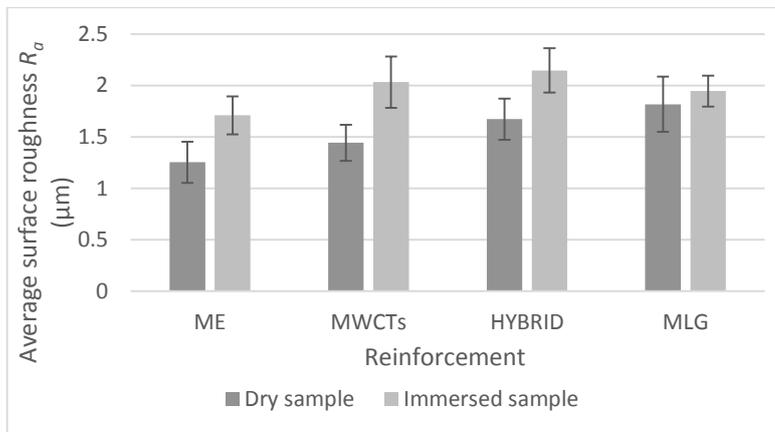

**Fig. 8. Average surface roughness of dry and immersed samples.**

3.5. SEM Images

Images of broken samples from tensile testing specimens were analysed using Scanning Electron Microscope (SEM) as shown in Fig. 9. This figure shows two distinctly different fracture surface of the epoxy sample. Smooth surface shows direct crack propagation whereas the rough surface shows a crack deflection mechanism. Crack bridging mechanisms were not visible in monolithic epoxy as in Fig. 9(a). When a crack started, it moves without any deviations and produces smooth fracture patterns.

When reinforcement was introduced, the surface roughness increased. This phenomenon can be associated with crack deflection mechanism formed from nano-filler reinforcement as shown in Fig. 9(b). Besides that, the improvement in surface roughness suggests an increase in the fracture path, which improved the stiffness and the strength of the nanocomposites. Figure 9(c) shows that the hybrid nanocomposites samples have higher surface roughness compared to monolithic epoxy and 0.1 wt% MWCNTs-epoxy. The samples did not show straight line brittle failure. Figure 10(d) shows that the 0.1 wt% MLG-epoxy has wrinkles and multilayers fracture on its

surface. Although hybrid nanocomposites caused an increase in tensile properties, the 0.1 wt% MLG-epoxy showed a more significant effect.

The uniformly-dispersed graphene can be achieved by adding a small amount of graphene. Homogenous dispersion of graphene provides good interfacial adhesion and resistance to crack propagation both in dry and wet condition. Additionally, the dispersed small amount of graphene in the matrix can form a continuous network, which could reduce stress concentration and bridge growing cracks, thus, stabilising and stopping the crack concentration.
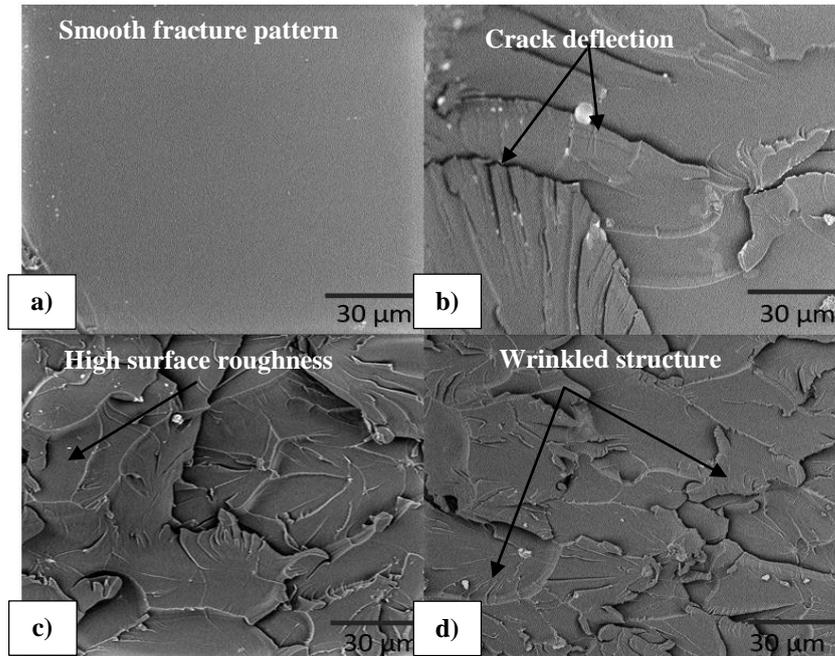
Fig. 9. SEM images of samples after water exposure; (a) monolithic epoxy, (b) 0.1 wt% MWCNTs-epoxy, (c) hybrid and (d) 0.1 wt% MLG-epoxy.

4. Conclusions

In conclusion, the mechanical properties of epoxy can be improved with the incorporation of 0.1 wt% MWCNTs, 0.05 wt% MWCNTs-0.05 wt% MLG and 0.1 wt% MLG. The Young's modulus of hybrid nanocomposites (0.05 wt% MWCNTs-0.05wt% MLG) increased up to 70%. In the case of 0.1 wt% MLG-epoxy nanocomposites, the Young's modulus improved 72.4%. After water exposure, the Young's modulus decreased for all nanocomposite systems. Compared to dry samples, the Young's modulus of monolithic epoxy decreased 9%. For hybrid samples, the Young's modulus decreased by 5.4% and in the case of 0.1 wt% MLG-epoxy, the Young's modulus dropped 6.7%. A similar trend was observed for tensile and impact strength, where all nanocomposite systems showed good improvement for samples tested in dry condition. It is worth to note that all nanocomposites were able to reduce water absorption due to the tortuosity effect. As a result, their mechanical properties were much better than monolithic epoxy. It can also be concluded that synergistic effects are not that effective at a low concentration of 0.1

wt % to cause a significant improvement in mechanical properties of produced nanocomposites. Graphene, however, has an impressive effect on the liquid barrier and mechanical properties of the nanocomposites. Nevertheless, more work needs to be carried out to fully understand the synergistic effect of MLG and MWCNTs at higher concentration. Further investigations in the characterisations, especially the dynamic mechanical properties are currently carried out and will be the subject of a forthcoming paper.

Nomenclatures	
$f(a/w)$	Calibration factor
K_{IC}	Fracture toughness
R_a	Average surface roughness
W_0	Initial weight of the sample
W_c	Final weight of specimen in %
W_t	Weight of specimen at time t
Abbreviations	
CNTs	Carbon Nanotubes
ME	Monolithic Epoxy
MLG	Multi-Layer Graphene
MWCNTs	Multi-Walled Carbon Nanotubes
SEN-TPB	Single Edged Notch-Three Point Bending

References

1. Guadagno, L.; Raimondo, M.; Vittoria, V.; Vertuccio, L.; Naddeo, C., Russo, S.; De Vivo, B.; Lamberti, P.; Spinelli, G., and Tucci, V. (2014). Development of epoxy mixtures for application in aeronautics and aerospace. *RSC Advances*, 4(30), 15474-15488.

2. Saharudin, M.S.; Atif, R.; Shyha, I.; and Inam F. (2016). The degradation of mechanical properties in polymer nano-composites exposed to liquid media - a review. *RSC Advances*, 6(2), 1076-1089.

3. Jakubinek, M.B.; Ashrafi, B.; Zhang, Y.; Martinez-Rubi, Y.; Kingston, C.T.; Johnston, A.; and Simard, B. (2015). Single-walled carbon nanotube-epoxy composites for structural and conductive aerospace adhesives. *Composites Part B: Engineering*, 69, 87-93.

4. Fischer, F.; Beier, U.; Wolff-Fabris, F.; and Altstädt, V. (2011). Toughened high performance epoxy resin system for aerospace applications. *Science and Engineering Composite Materials,*18(4), 209-215.

5. Yang, S.-Y.; Lin, W.-N.; Huang, Y.-L. Tien, H.-W.; Wang, J.-Y.; Ma, C.-C.M.; Li, S.-M.; and Wang, Y.-S. (2011). Synergetic effects of graphene platelets and carbon nanotubes on the mechanical and thermal properties of epoxy composites. *Carbon*, 49(3), 793-803.

6. Galpaya, D.; Wang, M.; Liu, M., Motta, N.; Waclawik, E.; and Yan, C. (2012). Recent advances in fabrication and characterization of graphene-polymer nanocomposites. *Graphene*, 1(2), 30-49.

7. Wajid, A.S.; Das, S.; Irin, F.; Ahmed, H.S.T.; Shelburne, J.L.; Parviz, D., Fullerton, R.J.; Jankowski, A.F.; Hedden, R.C.; and Green, M.J. (2012).

Polymer-stabilized graphene dispersions at high concentrations in organic solvents for composite production. *Carbon*, 50(2), 526-534.

8. Zhou, J.; and Lucas, J.P. (1995). The effects of a water environment on anomalous absorption behavior in graphite/epoxy composites. *Composites Science and Technology*, 53(1), 57-64.

9. Bunch, J.S.; Verbridge, S.S.; Alden, J.S.; van der Zande, A.M.; Parpia, J.M.; Craighead, H.G.; and McEuen, P.L. (2008). Impermeable atomic membranes from graphene sheets. *Nano Letters*, 8(8), 2458-2462.

10. Wei, J.; Saharudin, M.S.; Vo, T.; and Inam, F. (2017). Dichlorobenzene: an effective solvent for epoxy/graphene nanocomposites preparation. *Royal Society Open Science*, 4(10), 1-9.

11. Saharudin, M.S.; Shyha, I.; and Inam, F., (2016). Viscoelastic and mechanical properties of multi-layered-graphene polyester composites. *Proceedings of the 2nd International Conference on Advances in Mechanical Engineering.* Istanbul, Turkey, 41-45.

12. Saharudin, M.S.; Atif, R.; and Inam, F. (2017). Effect of short-term water exposure on the mechanical properties of halloysite nanotube-multi layer graphene reinforced polyester nanocomposites. *Polymers*, 9(1), 1-18.

13. Wei, J.; Saharudin, M.S.; Vo, T.; and Inam, F. (2017). N,N-Dimethylformamide (DMF) usage in epoxy/graphene nanocomposites: problems associated with reaggregation. *Polymers*, 9(1), 1-12.

14. Atif, R.; Shyha, I.; and Inam, F. (2016). The degradation of mechanical properties due to stress concentration caused by retained acetone in epoxy nanocomposites. *RSC Advances*, 6(41), 34188-34197.

15. Peeterbroeck, S.; Alexandre, M.; Nagy, J. B.; Pirlot, C.; Fonseca, A.; Moreau, N.; Philippin, G.; Delhalle, J.; Mekhalif, Z.; Sporken, R.; Beyer, G., and Dubois, P. (2004). Polymer-layered silicate-carbon nanotube nanocomposites: unique nanofiller synergistic effect. *Composite Science and Technology*, 64(15), 2317-2323.

16. Endo, M.; Strano, M.S.; and Ajayan, P.M. (2008). Potential applications of carbon nanotubes. *Carbon Nanotubes*, 111, 13-62.

17. Ajayan, P.M.; and Zhou, O.Z. (2001). Applications of carbon nanotubes. *Carbon Nanotubes*, 80, 391-425.

18. Inam, F.; and Luhyna, N. (2012). Carbon nanotubes for epoxy nanocomposites : A review on recent developments. *Proceedings of the 2nd* International *Conference on Advanced Composite Materials and Technologies for Aerospace Applications.* Wrexham, United Kingdom, 80-86.

19. Inam, F.; Wong, D.W.Y.; Kuwata, M.; and Peijs, T. (2010). Multiscale hybrid micro-nanocomposites based on carbon nanotubes and carbon fibers. *Journal of Nanomaterials*, Article ID 453420, 12 pages.

20. Saharudin, M.S.; Shyha, I.; and Inam, F. (2015). The effect of methanol exposure on the flexural and tensile properties of halloysite nanoclay polyester. *Proceedings of the IRES 17th International Conference.* United Kingdom. London, 40-44.

21. Sumfleth, J.; de Almeida Prado, L.A.S.; Sriyai, M.; and Karl, S. (2008). Titania-doped multi-walled carbon nanotubes epoxy composites: Enhanced

dispersion and synergistic effects in multiphase nanocomposites. *Polymer*, 49(23), 5105-5112.

22. Yang, S.-Y.; Ma, C.-C. M.; Teng, C.-C.; Huang, Y.-W.; Liao, S.-H.; Huang, Y.-L.; Tien, H.-W.; Lee, T.-M.; and Chiou, K.-C. (2010). Effect of functionalized carbon nanotubes on the thermal conductivity of epoxy composites. *Carbon*, 48(3), 592-603.

23. Liao, S.-H.; Yen, C.-Y.; Hung, C.-H.; Weng, C.-C.; Tsai, M.-C.; Lin, Y.-F.; Ma, C.C.M.; Pan, C.; and Su, A. (2008). One-step functionalization of carbon nanotubes by free-radical modification for the preparation of nanocomposite bipolar plates in polymer electrolyte membrane fuel cells. *Journal of Materials Chemistry*, 18(33), 3993-4002.

24. Saharudin, M.S.; Rasheed, A.; Shyha, I.; and Inam, F. (2017). The degradation of mechanical properties in halloysite nanoclay - polyester nanocomposites exposed to diluted methanol. *Journal of Composite Materials*, 51(11), 38 pages.

25. Faruk, O.; Bledzki, A.K.; Fink, H.-P.; and Sain, M. (2012). Biocomposites reinforced with natural fibers: 2000-2010. *Progress in Polymer Science*, 37(11), 1552-1596.

26. Alamri, H.; and Low, I.M. (2012). Effect of water absorption on the mechanical properties of nano-filler reinforced epoxy nanocomposites. Materials *and Design,* 42, 214-222.

27. Bhattacharya, M. (2016). Polymer nanocomposites - A comparison between carbon nanotubes, graphene, and clay as nanofillers. *Materials (Basel)*, 9(4), 1-35.

28 Atif, R.; Shyha, I. and Inam, F. (2016). Mechanical, thermal, and electrical properties of graphene-epoxy nanocomposites - A review. *Polymers*, 8(8), 37 pages.

29. Cussler, E.L.; Hughes, S.E.; Ward, W.J.; and Aris, R. (1988). Barrier membranes. *Journal of Membrane Science*, 38(2), 161-174.

30. Fredrickson, G.H.; and Bicerano, J. (1999). Barrier properties of oriented disk composites. *The Journal of Chemical Physics*, 110(4), 2181-2188.

31. Liu, W.; Hoa, S.V.; and Pugh, M. (2005). Fracture toughness and water uptake of high-performance epoxy/nanoclay nanocomposites. *Composites Science Technology*, 65(15-16), 2364-2373.

32. Tan, B.; and Thomas, N.L. (2016). A review of the water barrier properties of polymer/clay and polymer/graphene nanocomposites. *Journal of Membrane Science*, 514, 595-612.

33. Cui, Y.; Kumar, S.; Kona, B.R.; and van Houcke, D. (2015). Gas barrier properties of polymer/clay nanocomposites. *RSC Advances*, 5(78), 63669-63690.

34. Sobrinho, L.L.; Ferreira, M.; and Bastian, F.L. (2009). The effects of water absorption on an ester vinyl resin system. *Materials Research*, 12(3), 353-361.

35. Zabihi, O.; Ahmadi, M.; Nikafshar, S.; Preyeswary, K.C.; and Naebe, M. (2018). A technical review on epoxy-clay nanocomposites: Structure, properties, and their applications in fiber reinforced composites. *Composites Part B Engineering*, 135, 1-24.

36. Zainuddin, S.; Hosur, M.V.; Zhou, Y.; Kumar, A.; and Jeelani, S. (2009). Durability studies of montmorillonite clay filled epoxy composites under

different environmental conditions. *Materials Science and Engineering: A*, 507(1-2), 117-123.

37. Chhetri, S.; Adak, N.C.; Samanta, P.; Murmu, N.C.; Hui, D.; Kuila, T.; and Lee, J.H. (2018). Investigation of the mechanical and thermal properties of l-glutathione modified graphene/epoxy composites. *Composites Part B: Engineering*, 143, 105-112.

38. Wei, J.; Atif, R.; Vo, T.; and Inam, F. (2015). Graphene nanoplatelets in epoxy system: Dispersion, reaggregation, and mechanical properties of nanocomposites. *Journal of Nanomaterials*, 16(1), 1-12.

39. Novoselov, K.S.; Fal′ko, V.I.; Colombo, L.; Gellert, P.R.; Schwab, M.G.; and Kim, K. (2012). A roadmap for graphene. *Nature*, 490(7419), 192-200.

40. Balandin, A.A.; Ghosh, S.; Bao, W., Calizo, I.; Teweldebrhan, D.; Miao, F.; and Lau, C.N. (2008). Superior thermal conductivity of single-layer graphene. *Nano Letters,* 8(3), 902-907.